Measurement of the infrared photodetachment cross section of NO^-

Mohammad Al-Za'al, Harold C. Miller, and John W. Farley
Physics Department and Chemical Physics Institute, University of Oregon, Eugene, Oregon 97403
(Received 9 August 1985)

We have measured the infrared photodetachment cross section of the negative molecular ion NO^- for photons in the range 3000–4150 cm^{-1} (0.372–0.514 eV), using a coaxial ion-beam–laser-beam apparatus. The cross section declined by 56% as the photon energy increased. There was no evidence for an expected threshold in the cross section near 4000 cm^{-1} from the channel $NO(v'=2) \leftarrow NO^-(v''=0)$. This surprising result awaits theoretical interpretation.

INTRODUCTION

Photodetachment of negative molecular ions was first studied in the laboratory by Branscomb and others[1] before the invention of the laser. New laser-based techniques have increased the number of molecular ions that can be studied. The coaxial laser-beam–ion-beam geometry, first used by Wing *et al.*[2] to measure the infrared rotational-vibrational spectrum of HD^+, maximizes the overlap region, compared with experiments employing a crossed ion- and laser-beam geometry. A coaxial-beams apparatus with a visible dye laser has been used by Schulz *et al.*[3] to study OH^-, by Hefter *et al.*[4] to study C_2^-, and by Lykke *et al.*[5] to study FeO^- and $H_2C^-CHO^-$. Yet there have been very few coaxial-beams laser-based studies in the infrared. Instead, experiments with crossed beams and conventional light sources have followed in the Branscomb tradition.[6]

The molecular ion NO^- is a "clean" molecular system: only the ground vibrational state is stable against autodetachment. Consequently there are no vibrational hot bands. In this paper we review previous work on NO^-. We describe the experimental apparatus and our results. We discuss the theoretical behavior of the photodetachment cross section, using an adaptation of a simple semiempirical approach used for negative atomic ions. Finally, we discuss the disagreement between theory and experiment.

PREVIOUS WORK ON NO^-

Massey[7] provides a good general introduction to work on negative ions, including NO^-. Molecular constants and references to work published as of 1977 are given in the compendium by Huber and Herzberg.[8] Table I lists molecular constants for NO^- and NO.

The NO^- ion has been the subject of two major experimental studies. The first such study was performed by Spence and Schulz[9] in an electron scattering experiment on NO. A monoenergetic electron beam traversed a cell of NO, and the "trapped-electron" method was employed to measure the cross section for inelastic electron scattering as a function of electron energy. The experimental design reduced the background of elastically scattered

TABLE I. Molecular constants for the lowest electronic states of NO^- ($^3\Sigma^-$) and NO ($^2\Pi$). Data marked with an asterisk were not measured or calculated in the reference; rather they were assumed by the authors of that reference. 1 eV = 8065.5 cm^{-1}. EA denotes electron affinity. PD stands for photodetachment, ES for electron scattering, and CD for collisional detachment.

EA (meV)	ω_e (cm^{-1})	$\omega_e x_e$ (cm^{-1})	R_e (Å)	B_e (cm^{-1})	D_e (eV)	Expt. or theor.	Experimental technique	Ref.
				NO^-				
24^{+10}_{-5}	1470±200	8±2	1.258±0.010	1.427±0.002		expt.	PD	10
54*	1371	16±4	1.286			expt.	ES	9
	1371.1	8				expt.	ES	17
25	1331					expt.	ES	15
50±10	1363	8				expt.	ES	18
1200*[a]	1532	12	1.34		6.5	theor.		23
24*	1367±36	9±3	$1.267^{+0.004}_{-0.025}$			theor.		22
28							CD	19
				NO				
	1904.04	14.100	1.150 77	1.720 16				8
	1904.20	14.075		1.671 95				

[a]This value was assumed in an adjustment of all NO^- levels in order to match the calculated and experimental values of the separated-atom limit. Before adjustment the EA was 5.8 eV.

electrons to a level below the inelastic background. Resonances were observed in the cross section, superimposed on a rising inelastic background. The resonances correspond to energies of unstable (autodetaching) states of NO^-. The ground ($v=0$) vibrational level of NO^- was not observed, because it lies below the ground vibrational level of NO, and would therefore require a negative kinetic energy of the incoming electron. The widths of the resonances result from the autodetaching lifetimes of the vibrationally excited states of NO^-, and from the electron-beam energy width of 65 meV. Analysis of the data yielded the internuclear separation and vibrational spacings for the ion and neutral.

The second major study of NO^- was performed by Siegel *et al.*[10] using photoelectron spectrometry. A beam of NO^- was photodetached by an intracavity 488-nm Ar^+ laser beam in a crossed-beam geometry. The energy spectrum of the photodetached electrons was measured by an electrostatic energy analyzer. Transitions between $NO(v')$ and $NO^-(v'')$ were observed for $v'=0$–6. Only transitions involving $v''=0$ were observed, because the population of levels with $v''>0$ autodetaches too rapidly to survive the flight from the ion source to the interaction region. The analysis of the electron spectrometric data yielded the electron affinity of NO and a plethora of molecular constants for NO^-: Franck-Condon factors for the photodetachment process, vibrational and rotational constants, and the internuclear separation. This is the most complete previous work on NO^-, and we refer to it repeatedly below. For brevity we call it the Siegel study.

In addition to these two studies, which are most relevant to our experiment, there have been a number of other studies, which we mention briefly. Many of them involve excited electronic states of NO^-. We discuss first the studies employing the electron scattering technique.

Sanche and Schulz,[11] in an electron transmission experiment on NO, found Feshbach resonances between 5 and 7.5 eV, and interpreted them as resulting from a "grandparent" NO^+ core with two bound electrons. A later report by the same authors[12] included results on H_2, D_2, O_2, NO, N_2, and CO. All data were taken at electron energies in the range 5–20 eV. A related theoretical interpretation of the resonances found near 5 eV was given by Lefebvre.[13] A review article by Schulz[14] summarizes the results of a number of electron scattering experiments.

In other electron scattering experiments, Burrow[15] measured electrons scattered in collisions with NO. He detected electrons which scattered elastically through 180°, using a magnetic field to make this direction experimentally accessible. He found resonances below 2 eV.

Carbonneau and Marmet[16] crossed an electron beam with an NO molecular beam, and detected ions with a mass spectrometer. This experiment only studied phenomena appearing above 12 eV; therefore, the ground state of NO^- was not involved. The interpretation of the results also used the NO^+ grandparent model.

Zecca *et al.*[17] made measurements of the total electron cross section for NO in the 0–10-eV energy range, without the confining magnetic field used by Burrow and by Spence. They found that the cross section is large near zero electron energy. It decreases until the electron energy is about 0.15 eV, then increases with oscillations until about 1.2 eV. The increase in cross section as the energy decreases near zero energy is not an instrumental effect; Zecca *et al.* found a decrease in the electron scattering cross section on helium. Zecca *et al.* also looked at the transmitted electron current. The vibrational spacing in the range 0.15–1.2 eV was about 160 meV. In addition to the large resonances that were, in principle, understood from the work of Spence, they also found some unexplained "small sharp resonances."

The experiment of Tronc *et al.*[18] measured elastic and inelastic electron scattering on NO as a function of angle. They obtained a value for the electron affinity, the vibrational frequency of NO^-, and the anharmonicity. In contrast to the results of Spence and Schulz, their values for the autoionization widths of the peaks are constant at the experimental resolution of 40 meV, for all peaks with energies below 0.650 eV. Tronc *et al.* tried in vain to fit their data by assuming that the scattering is dominated by p waves, or d waves, or a mixture of both. They also found phenomena coincident in energy with the "small sharp resonances" found by Zecca *et al.*, and they attributed them to interference effects between two adjacent resonant peaks.

In addition to these electron-scattering experiments, there have been several more "chemical" experiments that rely on measurements of attachment and detachment rates. McFarland *et al.*[19] produced NO^- in a flowing afterglow with 0.2 Torr pressure. Under these conditions, they believe the reaction producing NO^- to be the following:

$$N_2O+e^-\rightarrow O^-+N_2$$

followed by

$$O^-+N_2O\rightarrow NO^-+NO\ .$$

McFarland *et al.* measured the collisional detachment rate constant for different values of temperature, and different buffer gases. They obtained a value for the electron affinity. Parkes and Sugden[20] measured detachment rates and attachment frequencies in a drift tube, and also obtained a measurement of the electron affinity. Finally, Chen and Wentworth[21] measured the electron affinity of NO using an electron-capture detector.

In contrast to the size of the experimental effort, there have been few papers on the theoretical side. Teillet-Billy and Fiquet-Fayard[22] analyzed the data of Tronc *et al.*[18] Theory analysis yielded the internuclear separation and vibrational constants. They found non-Franck-Condon effects for energies greater than 0.6 eV. These authors believed the autodetachment to proceed primarily via p-wave autodetachment, but with some d-wave autodetachment as well. They calculated the autodetachment widths to be all less than 40 meV. This agrees with Tronc's conclusions, and disagrees with the results of the Spence and Schulz experiment. These theoretical and experimental values for the autodetachment widths are listed in Table II. In another theoretical paper, Thulstrup *et al.*[23] performed an *ab initio* calculation of the energies of NO and

TABLE II. Autodetaching widths of vibrationally excited states of NO^- (meV).

$v=1$	$v=2$	$v=3$	$v=4$	T/E[a]	Ref.
25	35	50	65	E	9
40	40	40	40	E	18
1	5	10	15	T	22

[a] T denotes theoretical, E denotes experimental.

NO^-. The level of agreement with the experiment of Siegel *et al.* was not very good.

As this brief review shows, the NO^- ion has been the subject of many, often conflicting, studies. There have been no theoretical calculations of the frequency dependence of the photodetachment cross section.

APPARATUS

The apparatus used in this experiment comprises an ion beam machine, a color-center laser, and a detection system. A schematic of the apparatus is shown in Fig. 1.

Ion beam machine

The ion beam machine consists of an ion source, an extraction region, a Wien filter region, and an interaction region. All voltages on lens elements and deflectors are derived from two Power Designs[24] Model 1570 HV power supplies (± 3 kV, 40 mA), one operated at $+2$ kV and the other at -2 kV, using suitable chains of resistors and potentiometers.

The ion source

We use a hot-filament electrical discharge source of the type used by Branscomb.[25] The source gas, N_2O, is introduced to the source through Teflon tubing and pumped out through a 1-mm-diam aperture in the anode plate, which separates the source region from the extraction region. The pressure in the ion source is monitored in the extraction region, where the background pressure is 1×10^{-6} torr and the operating pressure is about 4×10^{-6} torr. The filament is a 2 mil$\times$27 mil thoriated-iridium ribbon[26] heated by a current of 5–6 A at about 4 V dc to produce electrons by thermionic emission.

The discharge voltage is about 50 V, producing an emission current of 2.5 mA. Three permanent magnets are placed around the source to confine the electrons. In order to stabilize the discharge, we constructed a regulator

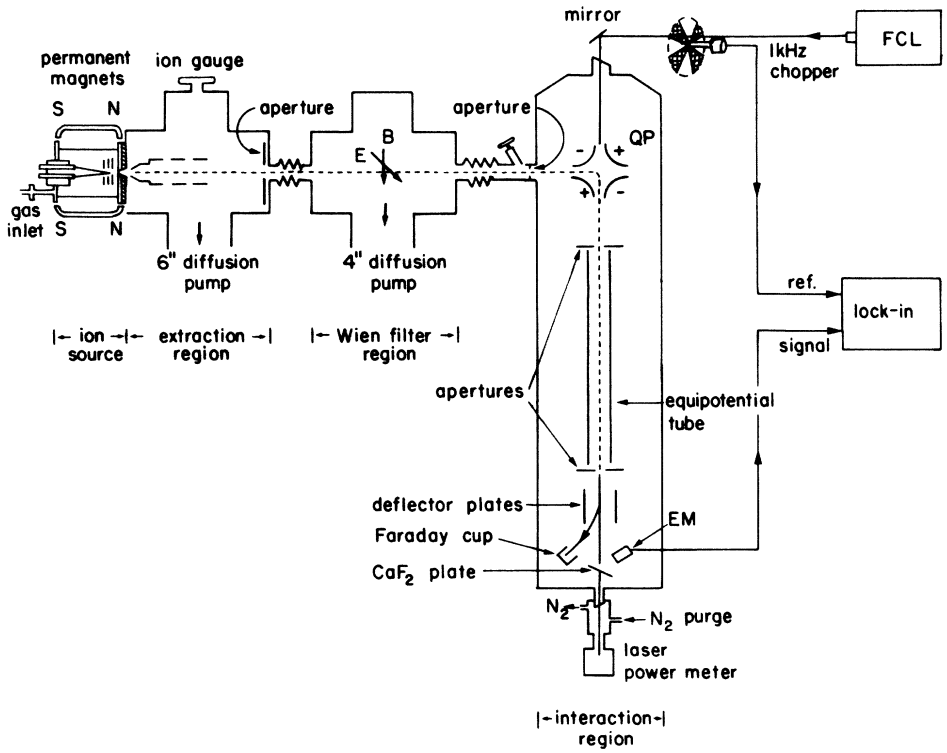

FIG. 1. Diagram of the coaxial ion-beam–laser-beam apparatus. A 2-keV beam of negative ions, produced in an active electrical discharge "Branscomb" source, is mass-selected by a Wien filter, deflected by an electrostatic quadrupole (QP), and overlapped coaxially by the infrared laser beam from a Burleigh FCL-20 color-center laser. After the laser beam detaches a portion of the ions, the charged particles are deflected into a Faraday cup. The fast neutrals collide with a CaF_2 plate, producing secondary electrons which are detected by an electron multiplier (EM). The laser beam is mechanically chopped, and the photodetachment is synchronously detected as a 1-kHz modulation in the fast neutral signal.

that adjusts the filament temperature to maintain constant emission current. The filament barely penetrates two floating "plasma-confining" aperture plates, which are mounted parallel to the anode plate and are separated by 3-mm glass spacers. Two millimeters from the tip of the filament is the spider plate, which is connected to the anode by 3.5-mm metal spacers. The spider plate has a triangular metal web at its center, determined by three circular holes, drilled at the vertices of an equilateral triangle centered on the beam axis. It shields the aperture from direct illumination from the filament, and provides a nearly field-free region in front of the aperture. The entire ion source assembly floats at -2 kV. Negative ions created in the vicinity of the aperture have 2 kV of kinetic energy after emerging from the source.

The extraction region

The ion lens used in this region consists of three cylindrical lens elements. The front end of the first element is cone-shaped and biased at about $+1100$ V in order to extract negative ions from the aperture in the anode plate. The second element is adjusted around -1400 V while the third element is grounded. The combination focuses the ion beam through a 1.5-mm aperture at the exist of the extraction region. Vertical and horizontal electrostatic deflectors are mounted on the same assembly to optimize the ion beam current into the Wien filter region.

Wien filter region

The Colutron[27] model 600 Wien filter consists of a parallel-plate capacitor and dual-coil iron-core electromagnet, which produces crossed electric and magnetic fields E and B. Only ions for which electric and magnetic forces cancel will pass through the filter. Since all ions emerging from the source have the same energy, ion species can be mass-selected by varying the magnetic coil current. Two einzel lenses located at the entrance and exit to the Wien filter focus the ions through a 1-mm aperture into the interaction region. The input lens is decelerating and biased at about -170 V, while the output lens is accelerating and biased near $+1600$ V. The background pressure in this region is about 1×10^{-6} torr and is essentially unchanged by the gas load from the ion source.

The interaction region

This region is a stainless-steel chamber whose pressure is maintained at about 2×10^{-9} torr by a 200 l/s ion pump. The ion beam entering through the entrance aperture is focused by an einzel lens and deflected at right angles by an electrostatic quadrupole.[28] The ions move along the axis of the chamber in a stainless-steel tube with a length of 50 cm and an inner diameter of 4 mm. The voltage on this "equipotential tube" can be varied allowing for high-resolution Doppler tuning of the ion beam. Ions emerging from the equipotential tube are deflected by an electrostatic deflector into a Faraday cup. The infrared laser beam enters this region through a CaF_2 Brewster window, travels along the axis of the chamber, overlapping the ion beam, and exists through a second CaF_2 Brewster window. The 2-kV neutral NO molecules resulting from photodetachment are not affected by the electrostatic deflector and strike a CaF_2 plate where they eject secondary electrons, which are collected and amplified by a Vacumetrics[29] Model AEM-1000 electron multiplier.

Color-center laser

A Burleigh model FCL-20 laser was used in the experiment. The lasing medium is a color-center crystal, pumped by an Ar^+ or Kr^+ laser. Depending on the wavelength, the peak laser power is between 4 and 30 mW, of which 35% survives the apertures of the interaction region.

Detection system

The output of the electron multiplier is fed to an electrometer with a 10 mV/nA conversion factor (10 MΩ equivalent resistance). The laser beam is chopped mechanically at about 1 kHz. An Ithaco model 391A lock-in amplifier employs phase-sensitive synchronous detection, with a time constant of 4 sec, to discriminate against neutrals resulting from collisional stripping by the background gas in the interaction region.

PROCEDURE

The current on each aperture is measured in order to monitor the ion beam and assist in alignment and focusing. The ion current collected by the Faraday cup (3—5 nA) is continuously monitored by an electrometer and a digital voltmeter.

The paths of both the ion and laser beams along the axis of the interaction chamber are defined by two 1.5-mm apertures located at the ends of the equipotential tube. The laser path is adjusted using two gold-plated mirrors to maximize the laser power through the interaction region, which is measured using a Scientech Model 36-2002 power meter. The power-meter head is coupled to the CaF_2 vacuum window through a Plexiglas tube, which is purged with dry nitrogen in order to eliminate any absorption effects due to atmospheric water vapor. A Burleigh WA-20IR Wavemeter, which can read either the wavelength (nm) or the frequency (cm^{-1}), is used to measure the laser frequency.

Voltages proportional to the neutral signal, ion current, and laser power are measured by the analog-to-digital converter (ADC) of an S-100-bus microcomputer. At fixed laser frequency, the computer samples the ADC inputs every 2 sec for 24 sec. The relative cross section was computed using the relation

$$Q = GLEI^{-1}P^{-1},$$

where Q is the relative cross section, G is the geometrical overlap factor between the ion beam and the laser beam, L is the lock-in signal, E is the photon energy, I is the ion current measured at the Faraday cup, and P is the laser power emerging from the interaction region. A value for the cross section was calculated every 2 sec, and the average values of all quantities were returned by a simple FOR-

TRAN program. Therefore, changes in I or P do not affect our measurement of Q.

A source of systematic error was variation in the geometrical overlap factor G. Such variation arose from two sources. First, changes in alignment of the laser beam as we changed the laser frequency; such changes are appreciable when the laser frequency changes by more than 200 cm^{-1}. A second and less important source of variation of G is slow drift in the direction of the ion beam. To minimize these effects, we adopted the following procedure: a number of separate scans were taken, each 100 cm^{-1} long, with data taken every 10 cm^{-1}. The laser beam was not realigned during each scan. Thus, the geometrical factor is essentially constant among points of a single scan.

Between scans, the laser beam is realigned in the ion beam apparatus to maximize the transmitted laser power. This keeps the geometrical overlap roughly constant across the entire frequency range of the laser. However, because the realignment procedure never reproduces exactly the same overlap, the result is a piecewise-continuous spectrum with small discontinuities between the 100-cm^{-1}-long scans. The discontinuities have been removed with a smoothing procedure: each scan has 20 cm^{-1} overlap with the adjacent scan. We multiply all points of a single scan by a common factor in order to produce agreement at the overlap points. This smoothing process makes small (few percent) adjustments in the data which are equally likely to be increases as decreases. Thus it is not a source of systematic error.

We have examined the possibility of another source of systematic error. If there were a systematic variation of the laser-beam divergence with laser frequency, then the laser power transmitted by the interaction region would not be a constant fraction of the laser power interacting with the ions. We have checked for this possibility by measuring the fraction of the laser power transmitted by the interaction region. We find that this fraction is constant over the laser frequency range within the accuracy of our measurement (3.8% rms) with no systematic increase or decrease.

In conclusion, the uncertainty in an individual data point arises from our inability to keep the geometrical overlap between ion beam and laser beam exactly constant as the laser frequency changes. This accounts for the scatter of the data about the smooth curve in Fig. 2.

RESULTS AND DISCUSSION

Our experimental results are shown in Fig. 2. The cross section declines smoothly as the laser wave number increases from 3000 to 4150 cm^{-1}, falling by over a factor of 2. This featureless experimental curve is actually quite surprising. In order to understand that, we must examine the theory briefly.

The relevant energy levels for NO^- and NO are shown in Fig. 3. In principle, there are two routes to photodetachment: direct detachment and resonant detachment. The direct detachment process is represented by the following equation, in which vibrationally excited states of NO^- do not play a role:

$$NO^-(v''=0)+h\nu \rightarrow NO(v')+e^- .$$

In contrast, the resonant photodetachment process is represented by a bound-bound transition in the ion,

$$NO^-(v'''=0)+h\nu \rightarrow NO^-(v'''>0) ,$$

followed by autodetachment,

$$NO^-(v'''>0) \rightarrow NO(v')+e^- .$$

These two different processes can give rise to the same final state. Therefore one should add the amplitudes, rather than the probabilities, for the two paths, in order to calculate the cross section theoretically.

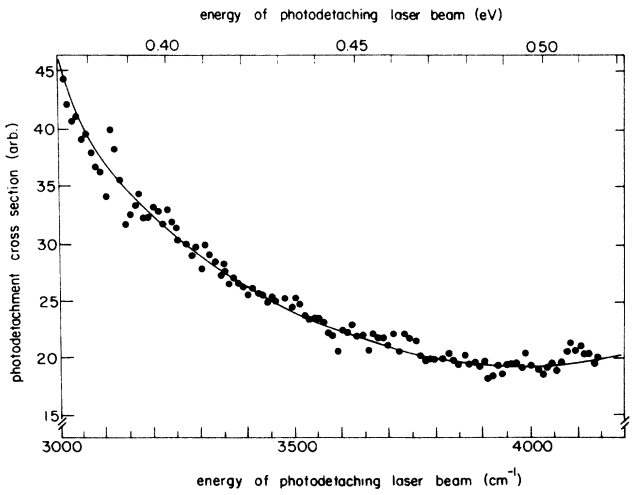

FIG. 2. The NO^- photodetachment cross section observed in this experiment. Note the offset in the vertical scale. The expected threshold for the $NO(v'=2) \leftarrow NO^-(v''=0)$ channel near 4000 cm^{-1} does not appear in the data. The decrease in the cross section from 3000 to 3800 cm^{-1} is interpreted as the 2-0 overtone transition in the ion, followed by autodetachment.

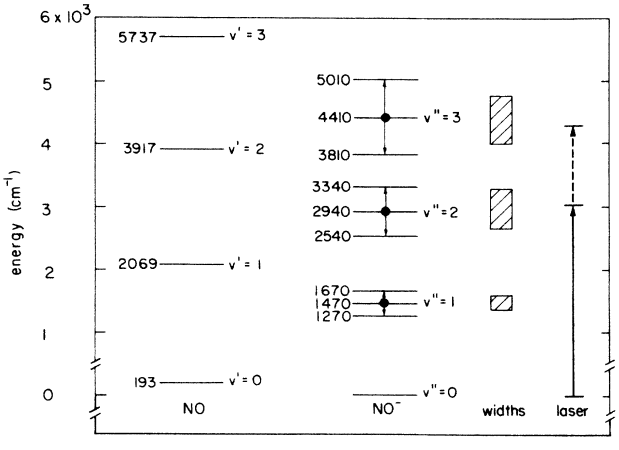

FIG. 3. Energy-level diagram of NO^- and NO, showing uncertainties, autodetachment widths of NO^- levels, and the energy range accessible to the FCL laser, exciting from the ground state of NO^-. The $v''=0$ state of NO^- is bound by 24 meV relative to $v'=0$ of NO. All vibrationally excited states of NO^- can autodetach.

We deal first with the resonant process. Theoretical calculation of the resonant contribution to the cross section is quite difficult and we will not attempt it. In the absence of strong interference effects between the resonant and nonresonant contribution, one expects the resonant contribution to be centered at the photon energy corresponding to the transition energy in the ion, with a width given by the autoionization lifetime of the excited state.

We deal next with direct (i.e., nonresonant) detachment. The photodetachment cross section Q for direct detachment is given by the following expression,[7] derived from Fermi's golden rule:

$$Q=(32\pi^4 m^2 e^2 v\nu/3hc^3)\,|\,\mathbf{M}\,|^2\,,$$

where $\mathbf{M}$ is the electric dipole matrix element

$$\mathbf{M}=\langle f,k\,|\,\mathbf{r}\,|\,i,h\nu\rangle\,.$$

In this expression, m is the electron mass, v is the final velocity of the departing electron, and ν is the laser frequency. The final state $|f,k\rangle$ is characterized by the neutral in state f and the detached electron having momentum $\hbar k$. The cross section decreases to zero at threshold because the phase space available to the departing electron vanishes. Below threshold, there is no final state available. Far enough above threshold, the cross section decreases because the wave function of the free electron oscillates much more rapidly than the wave function of the initial state, yielding cancellation. Roughly speaking, the maximum in the cross section occurs when the deBroglie wavelength of the free electron matches that of the bound electron. That means that the photon energy should be about twice the electron affinity.

Much theoretical effort has been devoted to calculating the detailed shape of the photodetachment cross section near threshold. In our case, it is more important to know the approximate shape of the photodetachment cross section over a wide range of photon energies, not necessarily near threshold. For these purposes, a different approach is needed.

We will assume that the matrix element can be written, following the Born-Oppenheimer approximation, as a product of electronic and vibrational factors

$$\mathbf{M}=\langle v_f\,|\,\langle f_e,k\,|\,\mathbf{r}\,|\,i_e,h\nu\rangle\,|\,v_i\rangle\,.$$

The inner electronic factor depends on the photon wavelength. Below threshold no final electronic state will exist. To a first approximation, the vibrational factors will not depend on the photon energy.

We assume that we can approximate the electronic part of the matrix element as the solution to a system without vibration; i.e., an atom. The vibrational factors are just the Franck-Condon factors.

In the Siegel study[10] it was assumed that the electronic part of the matrix element was constant with varying photon energy. That meant that the observed peak heights were simply proportional to the Franck-Condon factors. On that assumption, Siegel *et al.* derived values for the vibrational frequency and equilibrium internuclear distance by adjusting the molecular constants so the calculated Franck-Condon factors match the experimental resonance intensities. Their Franck-Condon factors are listed in Table III. Our approach is to model, in a simple way, the dependence of the electronic part of the matrix element.

Stehman and Woo[30] developed a simple physical model and semiempirical formulas for the shape of the photodetachment cross section of negative atomic ions. Their "zero-core-contribution" model (hereinafter, ZCC) is based on the following simplifying assumptions: (1) the wave functions of both the initial and final states can be approximately factored into the wave function of the neutral atomic core of radius r_0 and the wave function of the "extra electron" of angular momentum l; (2) the wave function of the atomic core is unchanged during the photodetachment process; and (3) the relevant electric dipole matrix element can be calculated by neglecting the contribution from the atomic core.

This approach was used earlier by Ohmura and Ohmura[31] to calculate the photodetachment cross section of H^-. Much earlier, Bethe and Longmire[32] used this "loosely bound approximation" to calculate the cross section for the photodisintegration of the deuteron.

These assumptions simplify the calculation by reducing the calculation of the matrix element to a one-electron problem. This model needs three parameters: the electron affinity, the core radius r_0, and the angular momentum of the orbital of the photodetaching electron. The ZCC model then yields an explicit analytical expression for the absolute photodetachment cross section as a function of photon energy.

The model fits the experimental cross sections quite well for several negative atomic ions: hydrogen and the alkali metals, carbon, and oxygen; and (somewhat less well) iodine. The model applies for several eV above threshold, not just near threshold.

The shape of the cross section depends on whether the detached electron comes from an s orbital or a p orbital. In the case of NO^-, which is isoelectronic to neutral O_2, detachment is from a p orbital. For the photodetachment of an electron from a p orbital we have

$$\sigma=\frac{8\pi e^2}{9\hbar c}\frac{m\omega k}{\hbar}(R_{sp}^2+2R_{dp}^2)\,,$$

where $\hbar k$ is the momentum of the departing electron and ω is the photon energy. R_{sp} and R_{dp} are given by

TABLE III. Franck-Condon factors for NO^- photodetachment at 488 nm, normalized to the 0-0 transition.

0-0	1-0	2-0	3-0	4-0	5-0	Source
1.0	2.54	2.57	1.4	0.4	0.2	Siegel (Ref. 10)
1.0	2.304	2.36	1.34	0.4	0.2	This work

$$R_{sp}=\frac{Ne^{-\gamma r_0}}{\gamma k(\gamma^2+k^2)}\left[\left[\frac{3\gamma^2k+k^3}{\gamma^2+k^2}+\gamma kr_0\right]\cos(kr_0)+\left[\frac{2\gamma^3}{\gamma^2+k^2}+\gamma^2r_0\right]\sin(kr_0)\right]$$

and

$$R_{dp}=-Ne^{-\gamma r_0}\left[\left[\frac{k^4+6\gamma^2k^2+3\gamma^4}{\gamma k^2(\gamma^2+k^2)^2}+\frac{r_0}{\gamma^2+k^2}\right]\cos(kr_0)-\left[\frac{3}{\gamma k^3r_0}+\frac{3k^2+\gamma^2}{k(k^2+\gamma^2)^2}-\frac{\gamma r_0}{k(\gamma^2+k^2)}\right]\sin(kr_0)\right].$$

Here $N^2=2\gamma e^{2\gamma r_0}/(1+2/\gamma r_0)$. The variable γ is given by $\gamma=\sqrt{2mE}/\hbar$ where E is the electron affinity.

The question arises as to what to use for the effective core radius r_0 for NO; from the Stehman paper,[30] we have for atomic oxygen, $r_0=0.96$ Å. This figure is $1.3R_{\rm rms}$, where the rms expectation value for R for the outermost occupied orbital is calculated by a Hartree procedure.[33] The factor of 1.3 was chosen by Stehman and Woo for all ions, to optimize the fit. The corresponding value for N is 1.11 Å. From Table I, the equilibrium internuclear separation R_e for neutral NO is 1.15 Å.

The question is how to combine the values for N, O, and the equilibrium internuclear separation for NO (0.96, 1.11, and 1.15 Å, respectively) to obtain a value for NO. We have done the calculation for three possible values: (1) naively using the equilibrium internuclear separation 1.15 Å; (2) using the largest plausible value, by taking $R(\mathrm{N})+R(\mathrm{O})-\frac{1}{2}R_e(\mathrm{NO})=1.495$ Å; and (3) using the smallest plausible value, using the oxygen value of 0.96 Å. This is physically plausible because the extra electron spends most of its time on the oxygen atom anyway.

TABLE IV. Effective electron affinity (EA) of the $\mathrm{NO}(v',J')\leftarrow\mathrm{NO}^-(v''=0,J'')$ transition for various values of v', and the calculated electron cross section in Å^2, using the ZCC model. The r_0 is 1.15 Å. The photon energy is 2.54 eV (wavelength of 488 nm).

v'	EA (eV)	Cross section (Å^2)
0	0.0417	0.137
1	0.2768	0.151
2	0.5072	0.149
3	0.7319	0.143
4	0.9526	0.137
5	1.1701	0.133

We have calculated the cross section for the rotationally corrected electron affinity of 0.0417 eV, for these three plausible values of r_0. Apart from an overall normalizing factor, the three curves turn out to be very similar, differing only by a few percent at the most (see Fig. 4). Consequently, for the sake of definiteness we have chosen $r_0=1.15$ Å.

In order to calculate the electronic dipole matrix element, we have to know the effective electronic affinity of the transitions $\mathrm{NO}(v',J')\leftarrow\mathrm{NO}^-(v'',J'')$, averaged over the initial rotational states of the ion. This is provided by Table IV, column 3, of Siegel, with a rotational correction of + 12.5 meV added. Entries for the (0-0) and (5-0) transitions have been added using information from Table I of Siegel. The result is shown in Table IV. The photon energy is 2.54 eV, corresponding to a wavelength of 488 nm.

The next step is to calculate the corrected Franck-Condon factors. For each transition, we divide the vibrational intensities observed by Siegel (Table III) by the calculated electronic cross section (Table IV) to obtain the

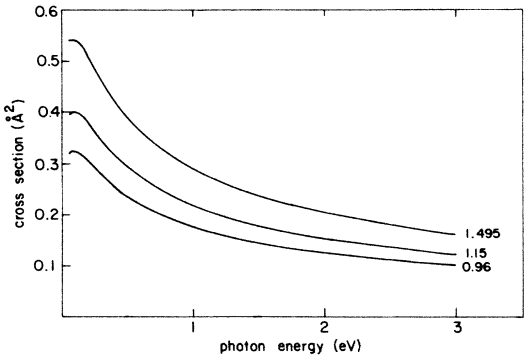

FIG. 4. Photodetachment cross section from an atomic p orbital as a function of photon energy. This curve is calculated using the "zero-core-contribution" approximation of Stehman and Woo (Ref. 30). The electron affinity was 24 meV. The core radius in angstroms is indicated. This demonstrates that the cross section decreases for photon energy much greater than about twice the electron affinity. The applicability of this atomic model calculation to a molecular system is discussed in the text. The three curves are very similar, apart from an overall normalization constant.

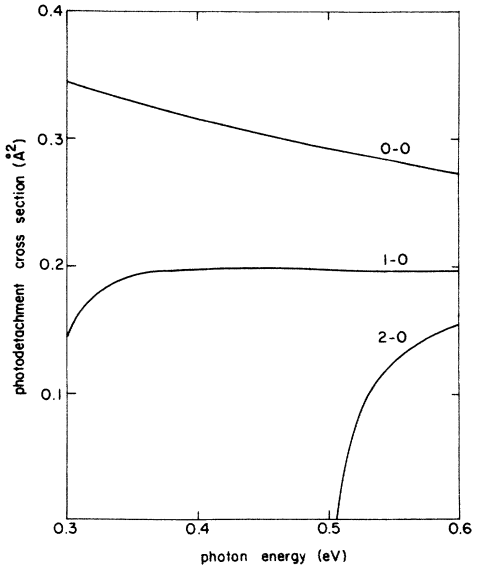

FIG. 5. Calculated electronic part of the photodetachment cross section for the $(v'=0,1,2\leftarrow v''=0)$ transitions, using the electron affinities in Table IV and the zero-core-contribution approximation. $R_e=1.15$ Å.

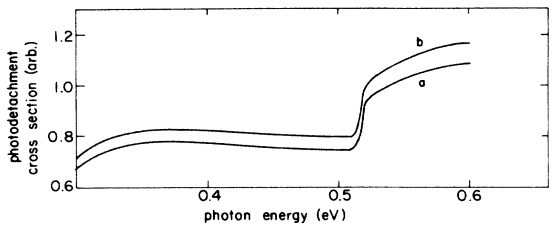

FIG. 6. Calculated total infrared photodetachment cross section for photons in the range 0.3—0.6 eV. Only the "direct" (i.e., nonresonant) contribution is included. (a) uses the corrected Franck-Condon factors, and (b) uses the Franck-Condon factors obtained by Ref. 10.

corrected Franck-Condon factors (Table III). The change is not important.

The next step is to calculate the vibrationally resolved cross sections in the infrared. Figure 5 shows the electronic part of the photodetachment cross section, for transitions ($v' \leftarrow v''=0$), using the electron affinities in Table IV.

In order to compare with experiment, we must sum over the final states. Our experiment is insensitive to the final state of the NO, because all fast neutrals with the same kinetic energy will have the same detection efficiency.

We calculate the observed cross section, obtained by summing the partial cross sections weighted by the Franck-Condon factors. Figure 6 shows the result using either corrected Franck-Condon factors or the Franck-Condon factors of Siegel.

A sharp threshold at 4000 cm^{-1} (0.5 eV) is expected, using either set of Franck-Condon factors. Thus there is an anomaly.

A second feature, easier to explain, is the large peak in Fig. 2 at small photon energy. Referring to Fig. 3, we see that there is an overtone transition (2-0) around 2940 cm^{-1}. The $v=2$ level of NO^- will then autodetach, yielding a fast neutral. If this interpretation is correct, we have a measurement of the autodetachment width of the $v=2$ level of NO^-. If the curve is assigned to be centered at 2940 cm^{-1}, and the "constant" background level visible at 4000 cm^{-1} is subtracted off, one obtains a full width at half maximum of 600 cm^{-1} (74 meV). Unambiguous measurement of the width will become possible only when measurements are made at lower photon energy to see the curve decrease again.

CONCLUSIONS

In this paper, we have analyzed the observed photodetachment cross section of NO^- in the 2—3 μm range. The curve is anomalous. This should not be too surprising. After all, the interpretation of the electron scattering experiment on NO has a long and contentious history, as our brief review of the literature shows. It is likely that the photodetachment question may be similarly complicated. Further progress depends on being able to shed new theoretical light on the question of the electronic part of the photodetachment cross section. The related problem of photoionization of O_2 (isoelectronic with NO^-) requires a full Hartree-Fock treatment.[34] It is likely that the interpretation of experimental data presented here will require a similarly sophisticated theoretical approach.

ACKNOWLEDGMENTS

We wish to acknowledge useful conversations with Paul Engelking and Barney Ellison. This work was supported by the Research Corporation, by the National Science Foundation under Grants No. PHY82-16889 and No. PHY85-02489, and by the Chemical Physics Institute of the University of Oregon.

[1]L. M. Branscomb, in *Atomic and Molecular Processes,* edited by D. R. Bates (Academic, New York, 1962), pp. 100—140.
[2]W. H. Wing, G. A. Ruff, W. E. Lamb, Jr., and J. J. Spezeski, Phys. Rev. Lett. **36**, 1488 (1976).
[3]P. A. Schulz, R. D. Mead, P. L. Jones, and W. C. Lineberger, J. Chem. Phys. **77**, 1153 (1982).
[4]U. Hefter, R. D. Mead, P. A. Schulz, and W. C. Lineberger, Phys. Rev. A **28**, 1429 (1983).
[5]K. R. Lykke, R. D. Mead, and W. C. Lineberger, Phys. Rev. Lett. **52**, 747 (1984).
[6]R. Rackwitz, D. Feldmann, E. Heinicke, and H. J. Kaiser, Z. Naturforsch. **29A**, 1797 (1974); R. Rackwitz, D. Feldmann, H. J. Kaiser, and E. Heinicke, *ibid.* **32A**, 594 (1977); D. Feldmann, *ibid.* **25A**, 621 (1970); D. Feldmann, R. Rackwitz, H. J. Kaiser, and E. Heinicke, *ibid.* **329**, 600 (1977).
[7]H. S. W. Massey, *Negative Ions* (Cambrdige University, Cambridge, England, 1976).
[8]K. P. Huber and G. Herzberg, *Constants of Diatomic Molecules* (Van Nostrand Reinhold, New York, 1979).
[9]D. Spence and G. J. Schulz, Phys. Rev. A **3**, 1968 (1971).
[10]M. W. Siegel, R. J. Celotta, J. L. Hall, J. Levine, and R. A. Bennett, Phys. Rev. A **6**, 607 (1972).
[11]L. Sanche and G. J. Schulz, Phys. Rev. Lett. **27**, 1333 (1971).
[12]L. Sanche and G. J. Schulz, Phys. Rev. A **6**, 69 (1972).
[13]H. Lefebvre-Brion, Chem. Phys. Lett. **19**, 456 (1973).
[14]G. J. Schulz, Rev. Mod. Phys. **45**, 423 (1973).
[15]P. D. Burrow, Chem. Phys. Lett. **26**, 265 (1974).
[16]R. Carbonneau and P. Marmet, Can. J. Phys. **52**, 1885 (1974).
[17]A. Zecca, I. Lazzizzera, M. Krauss, and C. E. Kuyatt, J. Chem. Phys. **61**, 4560 (1974).
[18]M. Tronc, A. Huetz, M. Landau, F. Pichou, and J. Reinhardt, J. Phys. B **8**, 1160 (1975).
[19]M. McFarland, D. B. Dunkin, F. C. Fehsenfeld, A. L. Schmeltekopf, and E. E. Ferguson, J. Chem. Phys. **56**, 2358 (1972).
[20]D. A. Parkes and T. M. Sugden, J. Chem. Soc., Faraday Trans. II **68**, 600 (1972).
[21]E. C. M. Chen and W. E. Wentworth, J. Phys. Chem. **87**, 45 (1983).
[22]D. Teillet-Billy and F. Fiquet-Fayard, J. Phys. B **10**, L111 (1977).
[23]P. W. Thulstrup, E. W. Thulstrup, and A. Andersen, J. Chem.

Phys. **60**, 3975 (1974).
[24]Power Designs, 1700 Shames Drive, Westbury, NY 11590.
[25]S. J. Smith and L. M. Branscomb, Rev. Sci. Instrum. **31**, 733 (1960).
[26]Electron Technology, 626 Schuyler Avenue, Kearney, NJ 07032.
[27]Colutron Corporation, 5420 Arapahoe Blvd., Boulder, CO 80303.
[28]J. W. Farley, Rev. Sci. Instrum. **56**, 1834 (1985).
[29]Vacumetrics, 2261 Palma Dr., Ventura, CA 93003.
[30]R. M. Stehman and S. B. Woo, Phys. Rev. A **20**, 281 (1979).
[31]T. Ohmura and H. Ohmura, Phys. Rev. **118**, 154 (1960).
[32]H. A. Bethe and L. Longmire, Phys. Rev. **77**, 647 (1950).
[33]C. C. Lu, T. A. Carlson, F. B. Malik, T. C. Tucker, and C. W. Nestor, Jr., At. Data **3**, 1 (1971).
[34]V. McKoy and R. Lucchese, *Electron-Molecule Collisional Photoionization Processes,* edited by V. McKoy, H. Suzuki, K. Takaganagi, and S. Trajmar (Chemie International, Deerfield Beach, Florida, 1983), pp. 13—20.